Acta Biochim Biophys Sin 2012, 44: 669–677 | © The Author 2012. Published by ABBS Editorial Office in association with Oxford University Press on behalf of the Institute of Biochemistry and Cell Biology, Shanghai Institutes for Biological Sciences, Chinese Academy of Sciences. DOI: 10.1093/abbs/gms049.
Advance Access Publication 21 June 2012

Original Article

Three-dimensional dynamic culture of pre-osteoblasts seeded in HA-CS/Col/nHAP composite scaffolds and treated with α-ZAL

Lu Liu[1,2†], Yong Guo[1†], Xuezhong Chen[3], Ruixin Li[1], Zhihong Li[1], Liang Wang[1], Zongming Wan[1], Jianyu Li[1], Qingxin Hao[1], Hao Li[1], and Xizheng Zhang[1*]

[1]Institute of Medical Equipment, Academy of Military Medical Sciences, Tianjin 300161, China
[2]Medical College, Chinese People's Armed Police Forces, Tianjin 300162, China
[3]Shenzhen Pingle Orthopaedic Hospital, Shenzhen 518000, China
[†]These two authors contributed equally to this work.
*Correspondence address. Tel: +86-22-84656717; Fax: +86-22-84656717; E-mail: zxz84656717@163.com

Pre-osteoblast MC3T3-E1 cells were cultured in hyaluronic acid-modified chitosan/collagen/nano-hydroxyapatite (HA-CS/Col/nHAP) composite scaffolds and treated with phytoestrogen α-zearalanol (α-ZAL) to improve bone tissue formation for bone tissue engineering. Perfusion and dynamic strain were applied to three-dimensional (3D) cultured cells, which simulates mechanical microenvironment in bone tissue and solves mass transfer issues. The morphology of cell-scaffold constructs *in vitro* was then examined and markers of osteogenesis were assessed by immunohistochemistry staining and western blotting. The results showed that cells expanded their pseudopodia in an irregular manner and dispersed along the walls in 3D-dynamic culture. Osteogenic phenotype was increased or maintained by enhanced collagen I (COLI) levels, decreased osteopontin expression and having little effect on osteocalcin expression during the 12 days of *in vitro* culture. In response to α-ZAL, the cell-scaffold constructs showed inhibited cellular proliferation, enhanced the alkaline phosphatase (ALP) activity and increased ratio of osteoprotegerin to receptor activator of nuclear factor kappa B (NF-κB) ligand (RANKL). Application of perfusion and dynamic strain to cells-scaffold constructs treated with α-ZAL represents a promising approach in the studies of osteogenesis stimulation of bone tissue engineering.

Keywords osteoblast; composite scaffold; α-zearalano; bioreactor; osteogenesis

Received: December 9, 2011 Accepted: April 16, 2012

Introduction

In vitro bone tissue engineering using biological materials often leads to poorly constructed extracellular matrix (ECM), unstable osteoblast adhesion and thus poor cell survival [1]. The quality of cell/material interactions affects the capacity of cell proliferation and differentiation [2]. Inadequate nutrient transmission also contributes to the failure of *in vitro* constructs [3]. Engineered bone does not have its own blood supply system, so the absorption of nutrient substances, transmission, and the excretion of wastes happen primarily through diffusion and penetration.

To overcome these difficulties, we modified biomaterials' surfaces to increase cellular adhesion and proliferation, and developed a bioreactor to imitate the living environment of osteoblasts. We have already described an organic–inorganic composite (hyaluronic acid-modified chitosan/collagen/nano-hydroxyapatite, HA-CS/Col/nHAP) made with amphiphilic materials, synthesized in our laboratory, and concluded that the composite is suitable for the growth of osteoblasts [4]. Chitosan (CS), a natural biodegradable polysaccharide with good biocompatibility and molding characteristics, has been widely used in the field of bone tissue engineering [5,6]. However, this polysaccharide's practical application is limited due to its poor hydrophilia. HA-modified CS can enhance surface invasion and increase cellular adhesion. nHAP, apart from the normal characteristics of HAP, forms very small particles, which not only enlarges the specific surface area but also increases surface roughness [7,8]. We have developed software and hardware for piezoelectric ceramic cell-loading device and built a new dynamic strain and circulating perfusion bioreactor system (**Fig. 1**) [9]. This device works well under appropriate 3D perfusion culture conditions and delivers an accurate compressive stimulus, which provides a reliable research platform for bone tissue engineering.

Cytokines, particularly growth factors, are important for tissue engineering. Growth factors, such as transforming growth factor beta (TGF-β) and bone morphogenetic protein-2 (BMP-2), improve bone formation *in vitro* [10]. However, estrogen is a promising candidate for bone

engineering. Estrogens increase osteoblast proliferation [11] and the production of many osteoblast proteins (e.g., insulin-like growth factor 1, type I procollagen, TGF-β, and BMP-6). Estrogens also suppress osteoclast activity *via* increased apoptosis and reduce osteoblast/stromal cell content of RANKL by the increased production of osteoprotegerin (OPG) [12]. Hong *et al.* [13] found that 17-beta estradiol improves osteogenic differentiation in 3D culture of human mesenchymal stromal cells. However, a wider practical application of 17-beta estradiol is limited because of its adverse clinical side effects. Here, we examined the effect of phytoestrogen α-ZAL on the growth of engineered bone tissue. α-ZAL, oomycetes phytoestrogen [chemical structure shown in **Fig. 2(A)**], is used in animal feed as a growth promoter, anabolic agent, and an estrogenic agent. Dai *et al.* [14] found that it has an anti-atherosclerotic effect similar to that of the endogenous estrogen 17-beta estradiol, whereas α-ZAL's effect on uterus and mammary gland proliferation is significantly lower. Previously, we determined the α-ZAL doses and regimens for the improvement of osteogenesis in 2D culture of pre-osteoblast MC3T3-E1 cells. It was found that α-ZAL inhibits osteoblast proliferation at the concentration of 10^{-6}–10^{-10} M but can induce osteogenic differentiation by increasing alkaline phosphatase (ALP) activity *in vitro* (data not shown).

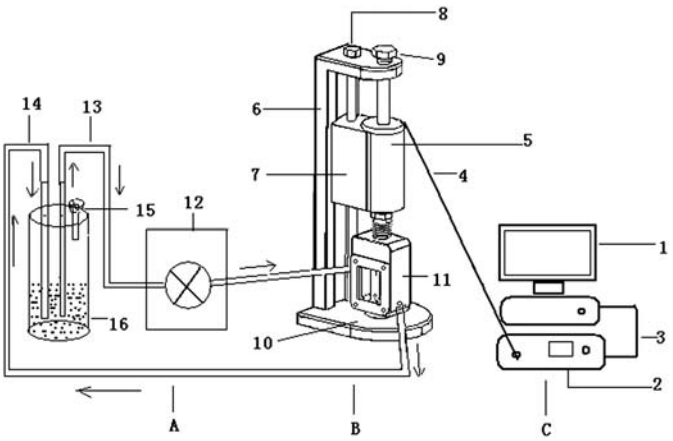

Figure 1 Structure diagram of dynamic strain and circulating perfusion bioreactor (A) Three-dimensional circulating perfusion system. (B) Piezoelectric ceramic loading device. (C) Loading power control systems. 1, host computer; 2, piezoelectric ceramic server; 3; data lines; 4, micro-displacement sensing signal line of; 5, piezoelectric ceramic element; 6, rigid frame; 7, sliding sleeve; 8, lifting screw; 9, fastening screw; 10, loading platform; 11, culture tanks; 12, peristaltic pump; 13, medium output pipe; 14, medium input pipe; 15, air filter; 16, medium tanks.

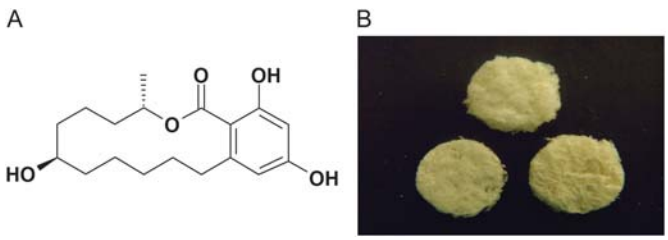

Figure 2 Chemical structure of α-ZAL (A) and external appearance of HA-CS/Col/nHAP composite scaffolds (B)

In this study, a 3D cell culture was used, employing HA-CS/Col/nHAP composite scaffold, dynamic strain, and circulating perfusion bioreactor. Scanning electron microscopy (SEM) was employed to evaluate cell phenotype. The differentiation markers of collagen I (COLI), osteopontin (OPN), and osteocalcin (OCN) were examined by immunohistochemistry and western blotting. Taking into account the results obtained for 2D cell culture with α-ZAL (the range10^{-6}–10^{-10} M), we investigated α-ZAL's effect on the cell proliferation, osteogenic differentiation and on the expression of OPG and RANKL in static and dynamic cultures.

Materials and Methods

Porous HA-CS/Col/nHAP composite scaffolds

The porous HA-CS/Col/nHAP blocks used in this study were made in our laboratory. This kind of scaffold is composed of modified CS, Col and nHAP [**Fig. 2(B)**]. The porosity of scaffold is 51% with a pore size ranging from 50 to 250 μm. The Young's modulus is 29.31 kPa. The scaffolds were molded into small cylindrical shapes with a radius of 5 mm and a thickness of 2–3 mm, and then sterilized by gamma irradiation at a dose of 25 kGy before cell seeding.

Cell culture and seeding of HA-CS/Col/nHAP composite scaffolds

The pre-osteoblast MC3T3-E1 cells (provided by Institute of Basic Medicine of Peking Union Medical College, Beijing, China) were seeded at a density of 10^4 cells/cm^2 in culture flasks with α-minimal essential medium (12571–048; Invitrogen, Carlsbad, USA) supplemented with 10% FBS (LC002; Sijiqing, Hangzhou, China) and 1% penicillin–streptomycin (SV30010; Hyclone, Logan, USA). The cells were cultured at 37°C in a humidified atmosphere of 95% air/5% CO_2. When cells reached 80% confluence, they were trypsinized and seeded on HA-CS/Col/nHAP scaffolds at a density of 10^6 cells/cm^3.

Application of dynamic strain and circulating perfusion to cell-scaffold constructs

Fluid shear stress and compressive stress was generated in the circulating perfusion and dynamic strain bioreactor [9]. Cell-scaffold constructs were placed in culture chambers, and subjected to fluid shear stress at flow rates of 5, 10, or 20 ml/min and compression strain of 3500 με, 1 Hz, 2 h/day. Unstrained (control) cultures were incubated under the same conditions. The cells were cultured for a required time, and then processed for SEM, histological, biochemical, or molecular analysis.

Treatment of 3D cultured cells with α-ZAL

MC3T3-E1cells were seeded on HA-CS/Col/nHAP scaffold at a density of 10^6 cells/cm^3 in 10 cm petri dishes. After 4 h, culture medium supplemented with 10^{-6}, 10^{-8}, or 10^{-10} M of α-ZAL (26538-44-3; Sigma, St Louis, USA) was added onto cells. The cells without α-ZAL treatment served as controls. After 24 h of incubation, the cell-scaffold constructs were transferred to culture chambers for dynamic culture at a flow rate of 10 ml/min and compression strain of 3500 με, 1 Hz, 2 h/day.

Scanning electronic microscopy

Samples of cell-scaffold constructs and of simple scaffold were fixed in 3% glutaraldehyde (24 h), 1% OsO_4 (1 h) and 2% tannic acid. They were then dehydrated in graded ethanol solutions, sputter-coated with gold/palladium. Images were examined and captured using a scanning electronic microscope (S-3400N; Hitachi, Ibaraki, Japan).

Hematoxylin and eosin staining

Samples of cell-scaffold constructs on days 1, 7, and 14 of incubation *in vitro* were fixed in 10% formaldehyde. After dehydration, the scaffolds were embedded in paraffin and sliced. Serial sections (5 μm) were cut and stained with hematoxylin and eosin (HE). Cell morphology and distribution were examined under a light microscope (Olympus, Tokyo, Japan).

Immunohistochemistry staining

Following deparaffinization, the sections were treated with 3% H_2O_2 and rinsed with deionized water. Next, the sections were incubated overnight with rabbit anti-COLI (BA0325, 1 : 200; Boster, Wuhan, China), rabbit anti-OPN (SC21742, 1 : 200; Santa Cruz, Santa Cruz, USA) and goat anti-OCN (SC23790, 1 : 200; Santa Cruz) antibodies at 4°C, and then rinsed three times with PBS. After incubation with biotin-conjugated anti-IgG (1 : 100; Santa Cruz), the sections were incubated with streptavidin-conjugated horseradish peroxidase, followed by incubation with diaminobenzidine (DAB) solution. Nuclei were counterstained with hematoxylin solution. Images were examined and captured using a light microscope (Olympus).

Western blot analysis

On days 3, 7, and 12, cell-scaffold constructs were solubilized in a modified radioimmunoprecipitation (RIPA) buffer (1% NP-40, 0.25% sodium deoxycholate, 150 mM NaCl, 1 mM EGTA, 1 mM phenylmethyl-sulfonyl fluoride, 1 mg/ml aprotinin, leupeptin, pepstatin, and 1 mM sodium orthovanadate in 50 mM Tris-HCl, pH 7.4). Protein samples (30 μg for COLI and OPN antibodies, or 60 μg for OCN antibody) were subjected to sodium dodecyl sulphate-polyacrylamide gel electrophoresis (SDS-PAGE) and then transferred onto nitrocellulose membranes. The mambranes were blocked by incubation in Tris-buffered saline with Tween-20 (TBS-T) with 5% milk for 1 h and probed overnight at 4°C with rabbit anti-COLI (1:300), rabbit anti-OPN (1:500) and goat anti-OCN (1:500) antibodies. After washing, the membranes were incubated with secondary antibody conjugated with horseradish peroxidase. The immunoreactive bands were visualized using enhanced chemiluminescence detection kit (SC2048; Santa Cruz). Optical density of the protein bands was determined with Gel Doc 2000 (Bio-Rad, Hercules, USA). The expression of GAPDH was used as a loading control and data were normalized to the corresponding GAPDH values.

Proliferation of 3D dynamically cultured MC3T3-E1 cells at different flow rates or with different concentrations of α-ZAL

We maintained the 3D dynamic cultures at different flow rates for 1, 3, 5, or 7 days or with different α-ZAL concentrations for 3 days. Then, the cell-scaffold constructs were placed in 24-well plates. Serum-free medium (600 μl) and cell counting kit-8 reagent (CCK-8) (CK04, 60 μl; Dojindo, Kumamoto, Japan) were added per well and incubated for 4 h at 37°C. Aliquots (150 μl) were transferred from 24-well plates to 96-well plates, and the absorbance was measured at 450 nm using a microplate reader (TECAN, Salzburg, Austria).

ALP activity assay

The 3D dynamic cultures were kept in different α-ZAL concentrations for 3 days. Then, cell-scaffold constructs were lysed in 500 μl/block of lysis buffer (10 mM Tris, pH 8.0, 1 mM $MgCl_2$, 0.5% Triton X-100), sonicated, and centrifuged to remove the cell debris and the scaffolds. ALP activity in the cellular fraction was measured by a spectrophotometric detection kit (A069-2; Jiancheng, Nanjing, China). ALP activity of each sample was normalized to protein concentration.

Expression of OPG and RANKL in 3D static and dynamic cultures of MC3T3-E1 cells with or without α-ZAL

Cell-scaffold constructs treated with 10^{-6} M α-ZAL were placed into culture chambers for dynamic culture for 7 days. Statically cultured constructs treated with 10^{-6} M of α-ZAL were used as controls. For dynamic cultures without α-ZAL constructs, a static culture without α-ZAL was used as a control. After 7 days, the constructs were solubilized in a modified RIPA buffer. Western blot analysis was used to measure the expression of OPG and RANKL (antibodies were rabbit anti-OPG and rabbit anti-RANKL, respectively, 30 μg of protein).

Statistical analysis

All experiments were performed in triplicate and repeated at least three times. Data were presented as the mean ± SD and analyzed with one-way analysis of variance to determine the significance between groups. Statistical analysis was performed using SPSS13.0 software (SPSS, Chicago, USA). $P < 0.05$ was considered statistically significant.

Results

Morphology of cell-scaffold constructs

The scaffold is a white, light, porous, sponge-like substance, as shown in **Fig. 2(B)**. SEM images demonstrate its internal structure [**Fig. 3(A,B)**]. The walls show layered distribution in the cross-section and pore-like in the longitudinal section; they are interconnected. The pore size in the scaffold is between 50 and 250 μm. The hydroxyapatite particles are well distributed and attached to the walls. Macropores help accommodate more cells and promote cell migration. **Figure 3(C)** shows cell morphology on the outer wall of the scaffold. Cells are of fusiform or irregular shape having extended pseudopodia, and secrete small amounts of fuzz or ECM, while cells inside the scaffolds tightly adhere to the walls or extend pseudopodia to connect across the pore's gap [**Fig. 3(D)**]. **Figure 3(E–G)** shows HE staining results. At the beginning of 3D dynamic culture, osteoblasts adhere to the pore walls [**Fig. 3(E)**]. They are round, without pseudopodia. As the culture continues, cells expand their pseudopodia

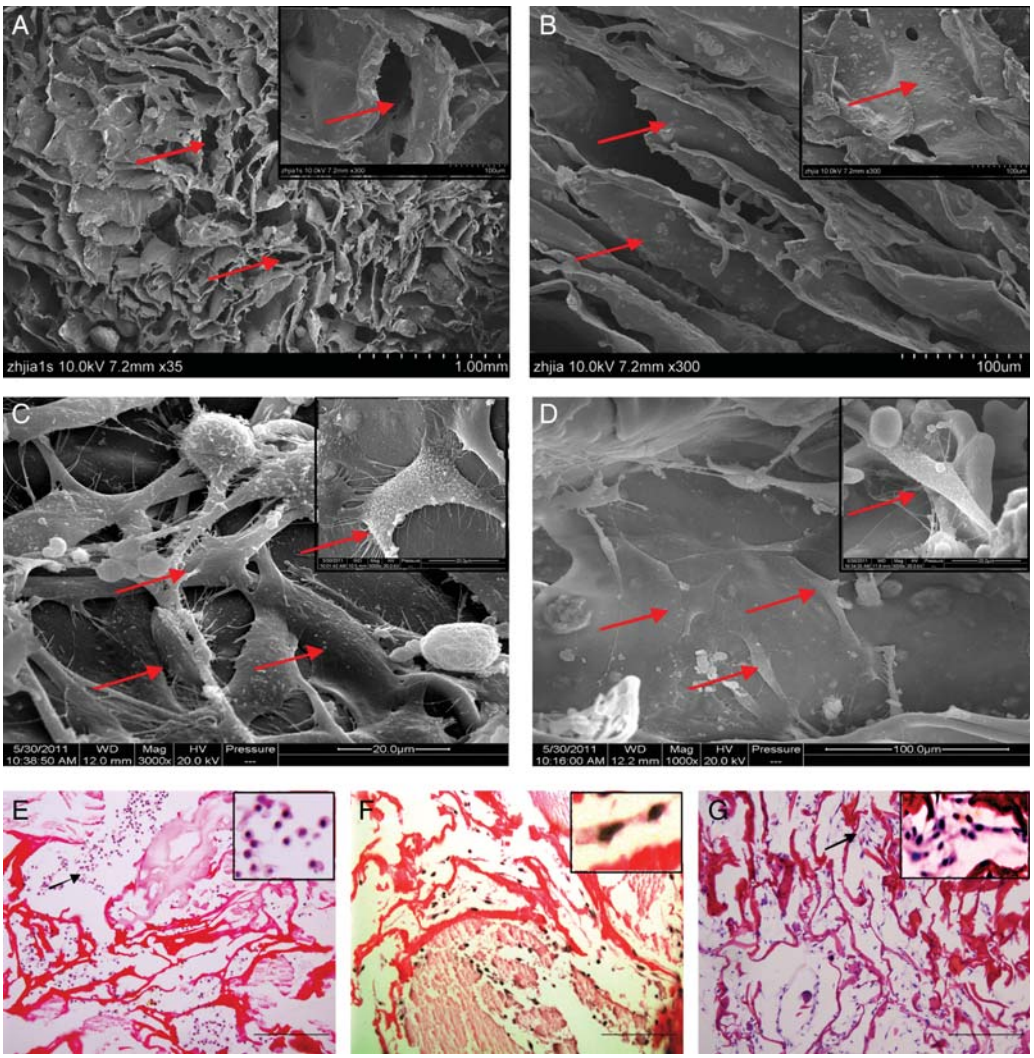

Figure 3 Morphology of MC3T3-E1 in 3D culture in HA-CS/Col/nHAP composite scaffolds (A) and (B) SEM of simple scaffold. (C) and (D) SEM of cell-scaffold constructs (5d). (E)–(G) HE staining of cell-scaffold constructs. Multiporous shapes can be seen on the simple scaffold in longitudinal section (A). Layered structure is visible in cross-section and nHAP disperses evenly on the pore wall (B). Cells adhere on the surface of scaffolds in fusiform or irregular shapes after 5 days of culture (C), have extended pseudopodia, and secrete small amounts of fuzz or ECM. Inside scaffold, cells adhere to the pore wall or extend pseudopodia connecting pore gaps (D). HE staining of cell-scaffold constructs is shown after 1 day (E), 7 days (F), and 14 days (G). At the beginning of *in vitro* culture, the cells were round, without pseudopodia (E). After 7 days of culture, the cells have irregular spindle shape and dispersed distribution (F). On day 14, cells grow in a colony-like manner (G). Bar = 100 μm.

in an irregular spindle manner and disperse along the walls. Nuclei and cytoplasm are clearly visible [**Fig. 3(F)**]. On day 14, cells grow in a colony-like manner [**Fig. 3(G)**].

Osteoblasts maintain osteogenesis in 3D dynamically cultured cell-scaffold constructs

Immunohistochemistry staining, spectrophotometric detection, and western blot analyses were performed to determine the expression of osteogenesis markers. The immunohistochemistry staining for three antibodies (anti-COLI, anti-OPN, and anti-OCN) was all positive. At the beginning of culture (day 1), both COLI and OPN display high expression levels [**Fig. 4(A,C)**] while OCN's expression is very low [**Fig. 4(E)**]. Up to day 7, brown areas appear in clusters around cellular nuclei for all the three antibodies [**Fig. 4(B,D,F)**]. Some appear beyond

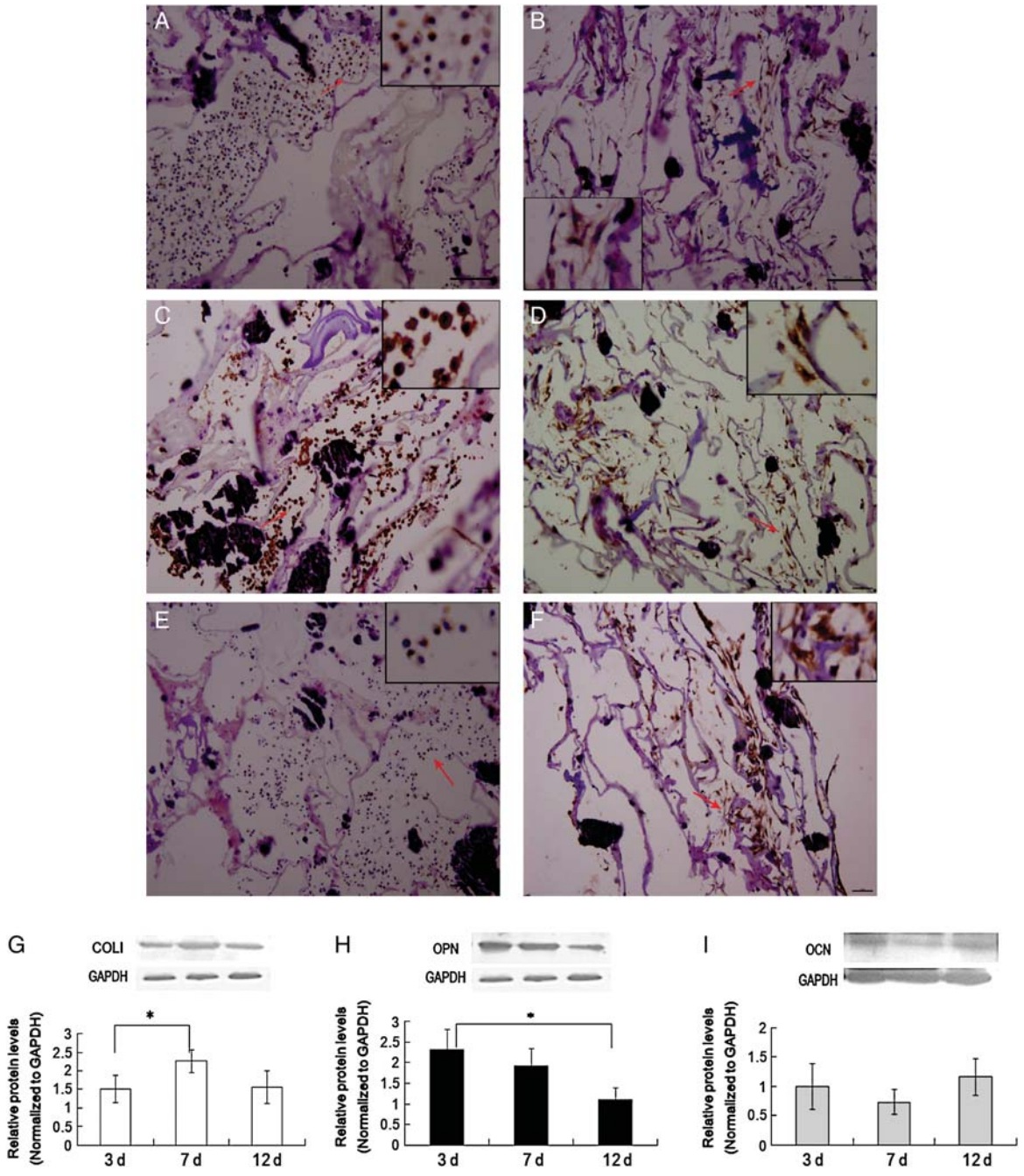

Figure 4 Immunohistochemistry staining and western blot analysis of cell-scaffold constructs *in vitro* On the first day of culturing, both COLI (A) and OPN (C) have high expression levels while expression of OCN is very low (E). Up to day 7, staining for all three antibodies were seen in clusters around cellular nuclei or near cellular membrane (B, D, F, brown area). Bar = 100 μm. Expression of COL 1 was up-regulated on day 7 (G), while expression of OPN was significantly down-regulated on day 12 (H). Expression of OCN did not change during the 12 days of *in vitro* culture (I). Results are shown as mean ± SD from three independent experiments. $^*P < 0.05$.

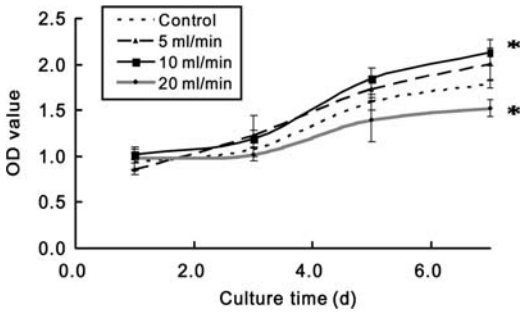

Figure 5 The effect of dynamic culture with different flow rates on proliferation of MC3T3-E1 cells Perfusion at 10 ml/min flow rate increases proliferation of MC3T3-E1 cells, while perfusion at 20 ml/min flow rate decreases cell proliferation. Data are presented as mean ± SD ($n = 4$) *$P < 0.05$ versus control.

cellular membrane, suggesting that osteoblasts cultured for 7 days *in vitro* begin to form ECM. COLI was significantly up-regulated on day 7 of culture compared with that on day 3. However, OPN expression significantly decreased over the observation period. The expression of OCN did not change during the 12 days of *in vitro* culture.

Dynamic culture at 10 ml/min flow rate promotes proliferation of MC3T3-E1 cells

Flow rate is a very important factor affecting dynamic culture. To determine the best culture conditions, we employed three flow speeds of 5, 10, and 20 ml/min with addition of compression strain of 3500 με to observe their effect on cell proliferation. After dynamic culturing for 1, 3, 5, and 7 days, cell-scaffold constructs were taken out of culture chambers and submitted to CCK-8 kit detection. As shown in **Fig. 5**, no differences were found for the first 3 days. By day 7, the number of cells in 10 ml/min flow rate group significantly increased ($P < 0.05$). The second best was 5 ml/min flow rate group. However, in 20 ml/min flow rate group significant decrease was observed ($P < 0.05$) and cell proliferation, indicating that shear stress at that flow rate is high enough to damage the cells.

High concentrations of α-ZAL inhibits cellular proliferation, but promotes ALP activity, of 3D dynamically cultured MC3T3-E1 cells

After we established 3D-culture model, we supplemented the cultures with α-ZAL to stimulate the growth of engineered bone tissue. We first determined the effect of α-ZAL on proliferation of MC3T3-E1 cells by CCK-8 assay. It was found that α-ZAL inhibits cell proliferation after 72 h of treatment at high concentrations (10^{-6} and 10^{-8} M), and 10^{-10} M of α-ZAL does not have significant effect on cell growth, as shown in **Fig. 6**. Next, we determined ALP activity by a fluorometric detection kit. ALP is an early differentiation marker for osteoblasts. As shown

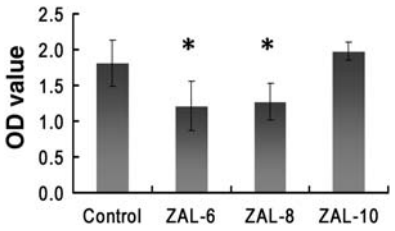

Figure 6 The effect of α-ZAL on proliferation of MC3T3-E1 cells α-ZAL at the concentration of 10^{-6} and 10^{-8} M inhibits cell proliferation. Data are presented as mean ± SD ($n = 4$) *$P < 0.05$ versus control.

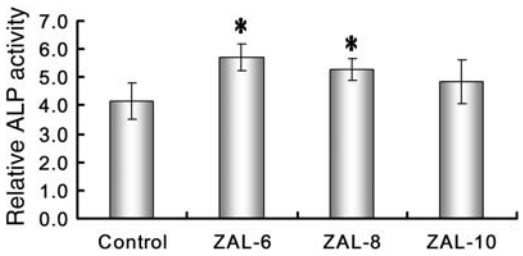

Figure 7 The auxoaction of α-ZAL on ALP activity of 3D-cultured MC3T3-E1 cells α-ZAL, at the concentration of 10^{-6} and 10^{-8} M, promotes ALP activity. Data are presented as mean ± SD ($n = 3$) *$P < 0.05$ versus control.

in **Fig. 7**, α-ZAL increased ALP activity in a dose-dependent manner.

α-ZAL increases OPG/RANKL ratio in 3D dynamic cultures of MC3T3-E1 cells

As shown in **Fig. 8**, both OPG and RANKL expression were significantly higher in the 3D static culture treated with α-ZAL than those without α-ZAL. OPG expression increased nearly 1.9-fold ($P < 0.05$), and RANKL also increased 1.9-fold ($P < 0.05$); the OPG/RANKL ratio did not change. In dynamic culture, OPG expression increased 1.3-fold ($P < 0.05$) in comparison with the control, and RANKL expression was slightly lower (OPG/RANKL ratio increased), suggesting that the dynamic culture of osteoblasts with α-ZAL favors osteogenesis, while 3D static culture does not. Next, we compared with static control and dynamic control to investigate the effect of mechanical strain alone on OPG and RANKL expression. Dynamic culture can significantly increase OPG and RANKL expression in osteoblasts when compared with static control. OPG expression increased 1.7-fold and RANKL expression increased 3.2-fold, so the OPG/RANKL ratio decreased.

Discussion

In this study, we used pre-osteoblast MC3T3-E1 cells in conjunction with HA-CS/Col/nHAP composite scaffolds, two different culture systems (static culture and dynamic

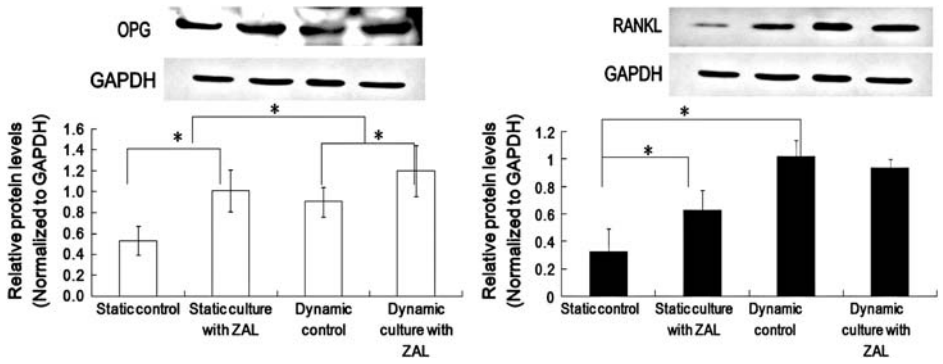

Figure 8 Expression of OPG and RANKL in MC3T3-E1 cells dynamically cultured for 7 days versus static culture with or without α-ZAL (10^{-6} M) α-ZAL promotes expression of both OPG and RANKL in comparison with static control. The increase in the expression of OPG was even more pronounced than that of RANKL. In the dynamic culture, α-ZAL promoted expression of OPG, but inhibited expression of RANKL in comparison with control. Flow rate was 10 ml/min, compression strain 3500 με, 1 Hz, 2 h/day. Results are presented as mean ± SD ($n = 3$). *$P < 0.05$ versus controls (static control or dynamic control).

culture), and phytoestrogen α-ZAL to study bone formation. The cell-scaffold and the bioreactor system which mimics some aspects of the physiological environment can be adopted in tissue development or control studies.

HA-CS/Col/nHAP composite scaffold imitates natural bone with good porosity and water absorption capacity. It can absorb cell suspension fast and thoroughly without being pre-soaked with PBS, thus promoting cell adhesion in the early culture period. The scaffold regulates cell phenotype which is rather different from the phenotype in 2D culture of pre-osteoblast MC3T3-E1. Cells tightly adhere to the wall of the scaffold, either on its outer wall or inside it. The immunohistochemistry staining also demonstrated that the osteoblasts maintain osteogenesis in HA-CS/Col/nHAP composite scaffolds. With the aid of bioreactor, cells enter the scaffold without cavitation.

Dynamic culture, replacing the traditional static culture, has become a new trend in bone tissue engineering [15]. However, the existing bioreactors for tissue engineering applications still have some problems. For example, spinner flasks or microcarrier reactors produce large shear forces and the fluid shear stress is difficult to control. Nutrient exchange varies widely between the culture surface and the internal scaffold [16]. In this study, we used dynamic strain and circulating perfusion bioreactor which had been designed for an effective simulation of bone microenvironment *in vivo*. Medium was delivered slowly through the pores in the scaffold by peristaltic pump, which not only improved mass transfer, but also supplied a certain amount of fluid shear stress. Fluid shear stress seems to have a dual effect: a high level of shear stress damages cells while a low stress improves cell growth and function [17,18]. Botchwey *et al.* [16] found that the cells seeded onto a microcarrier easily adhered to the scaffold at 3.9 dyne/cm^2 of shear stress, increased expression of ALP and maintained osteoblast phenotype. Goldstein *et al.* [19] reported that the exerted shear stress depends on many different factors, including porosity, pore size, and diameter of the scaffold, diameter of culture chamber, viscosity of culture medium, and flow rate. For a given scaffold and culture conditions, the fluid shear stress is directly proportional to flow rate. We could not calculate the exact value of fluid shear stress, and had to observe its effects through experiment. The optimal results were obtained for the flow rate of 10 ml/min; higher flow rate inhibits cell proliferation.

Osteogenic differentiation procedurally experienced gene expression of ALP, OPN, COLI, and OCN in a time-dependent manner. ALP and OPN are markers of early differentiation [20], while OCN is a late marker corresponding with matrix deposition and mineralization [21]. COLI is the most abundant protein in bone. Its expression is complexly regulated by a set of different factors [22]. In this study OPN showed a decrease expression after day 3 in our study which might reflect the transition from an early 'immature' stage to a more differentiated phenotype, as verified by the up-regulation of COLI under 3D dynamic condition after day 3, which is consistent with the common findings [23]. OCN expression did not change (12 days), indicating the condition of osteogenic differentiation was maintained. Such regulation illuminates the complex interactions and time-dependent expression of the 3D culture system.

We also investigated the effect of phytoestrogen α-ZAL on osteoblast proliferation and osteogenic differentiation. Phytoestrogens can be divided into five categories: isoflavones, lignans, chrysophenine, coumestrol, and those of fungal origin [24]. α-ZAL has been recently discovered in a fungus, *Gibberella zeae*. Researchers reported that phytoestrogens display a biphasic effect [25]: at the doses outside the optimal range (both at lower and higher doses) their positive effect is diminished, and inhibition of proliferation has been observed at very high doses [26]. In our study, it was found that α-ZAL, at high concentrations (10^{-6} and 10^{-8} M), inhibits cell proliferation of 3D

cultured MC3T3-E1 cells, but does not significantly affect cell growth at 10^{-10} M. α-ZAL promotes osteogenic differentiation by enhancing ALP activity at 10^{-6} and 10^{-8} M. OPG/RANKL ratio is a marker of bone formation reflecting the regulation of differentiation and activity of osteoclasts in the osteoblast lineage [27]. The results we obtained for the dynamic culture showed that α-ZAL enhances osteogenesis. This result is consistent with osteoblasts' response to other estrogens, confirming that α-ZAL can promote osteogenesis in a manner similar to 17-beta estrogen.

Various studies examining whether and how mechanical strain is involved in the regulation of OPG and RANKL expression provided mixed results. For example, Sanchez *et al.* [28] found that continuous mechanical loading decreased OPG expression in osteoblasts. Ludwika Kreja *et al.* [29] gave intermittent mechanical strain to human osteoblasts and found increased mRNA expression of RANKL. They also found that continuous loading had no significant effect on RANKL expression. The expression of OPG was not significantly influenced. Another study was focused on oscillatory fluid flow, in which Chi-adopted ST-2 murine bone marrow stromal cells and found a significant increase in OPG and decrease in RANKL with increasing load duration of up to 2 h [30]. This suggests that changes in OPG/RANKL ratio in response to mechanical forces depend on the context, cell types, mode of stress load, and magnitude of strain. In our study, mechanical forces (fluid shear stress and compressive stress) generated by bioreactor increased both OPG and RANKL expression, but in favor of RANKL, indicating such mechanical condition was not conducive to the inhibition of osteoclasts activity.

However, in our previous work with 2D cultures of MC3T3-E1, we found that α-ZAL inhibits osteoblast proliferation at the concentration of 10^{-6}–10^{-10} M and enhanced the activity of ALP and raised the ratio of OPG/RANKL mRNA at high concentrations (10^{-6} and 10^{-8} M) rather than at the low concentration of 10^{-10} M. It seems that cells grow differently in response to drug stimuli in 3D and 2D cultures. The reason maybe that cells are living in 3D ECM rather than in glass or plastic surface. This work has been pursued so as to provide biologically mimetic model systems. We believe that engineered bone tissue could be used as an efficient drug-screening platform. The 2D model commonly used for drug screening is only a poor topological approximation of the more complex 3D architecture of the ECM. A more realistic engineered tissue model is essential to reproduce physiological patterns of cell adherence, cytoskeletal organization, migration, and signal transduction [31]. Our engineered tissue could be a useful system to evaluate drugs' biological properties [32]. Optimizing 3D model to be used for drug screening, instead of animal models, will eliminate many practical problems and provide a bone microenvironment similar to *in vivo* conditions.

Funding

This work was supported by a grant from the National Nature Science Foundation of China (No. 10832012).

References

1 Lieb E, Milz S, Hacker M, Dauner M and Schulz MB. Effects of transforming growth factor-β1 on bonelike tissue formation in three-dimensional cell culture. J Tissue Eng 2004, 10: 1399–1413.
2 Anselme K. Osteoblast adhesion on biomaterials. Biomaterials 2000, 21: 667–681.
3 Ong SY, Dai H and Leong KW. Inducing hepatic differentiation of human mesenchymal stem cells in pellet culture. Biomaterials 2006, 27: 4087–4097.
4 Liu L, Li RX and Zhang L. Mechanical properties of hyaluronic acid modifying chitosan/collagen/nano-hydroxyapatite composite scaffold and its effect on osteoblast proliferation. Chin J Tissue Eng Clin Heal 2011, 15: 7127–7131.
5 Yi H, Wu LQ, Bentley WE, Ghodssi R, Rubloff GW, Culver JN and Payne GF. Biofabrication with chitosan. Biomacromolecules 2005, 6: 2881–2894.
6 De Souza R, Zahedi P, Allen CJ and Piquette-Miller M. Biocompatibility of injectable chitosan–phospholipid implant systems. Biomaterials 2009, 30: 3818–3824.
7 Chidambaram S, Sanghamitra B and Debabrata B. Studies on novel bioactive glasses and bioactive glass-nano-HAP composites suitable for coating on metallic implants. J Ceramics Int 2011, 37: 759–769.
8 Sundaram CS, Viswanathan N and Meenakshi S. Fluoride sorption by nano-hydroxyapatite/chitin composite. J Hazard Mater 2009, 172: 147–151.
9 Chen XZ, Shi CH and Li RX. A design of a new dynamic load and circulating-perfusion bioreactor system. Tissue Eng 2004, 10: 1399–1413.
10 Lieb E, Milz S, Vogel T, Hacker M, Dauner M and Schulz MB. Effects of transforming growth factor-β1 on bonelike tissue formation in three-dimensional cell culture. Tissue Eng 2004, 10: 1399–1413.
11 Fujita M, Urano T, Horie K, Ikeda K, Tsukui T, Fukuoka H and Tsutsumi O, *et al*. Estrogen activates cyclin-dependent kinases 4 and 6 through induction of cyclin D in rat primary osteoblasts. Biochem Biophys Res Commun 2002, 299: 222–228.
12 Syed F and Khosla S. Mechanisms of sex steroid effects on bone. Biochem Biophys Res Commun 2005, 328: 688–696.
13 Hong L, Krishnamachari Y, Seabold D, Joshi V, Schneider G and Salem AK. Intracellular release of 17-beta estradiol from cationic polyamidoamine dendrimer surface-modified poly (lactic-co-glycolic acid) microparticles improves osteogenic differentiation of human mesenchymal stromal cells. Tissue Eng Part C Methods 2011, 17: 319–325.
14 Dai SL, Duan J and Lu Y. A new phytoestrogen α-Zearalanol markedly inhibits progression of atherogensis in overiectomized cholesterol – fed rabbits. J Mol Cell Cardiol 2002, 34: 24–27.
15 Lujan TJ, Wirtz KM, Bahney CS, Madey SM, Johnstone B and Bottlang M. A novel bioreactor for the dynamic stimulation and mechanical evaluation of multiple tissue-engineered constructs. Tissue Eng Part C Methods 2011, 17: 367–374.

16 Botchwey EA, Pollack SR, Levine EM and Laurencin CT. Bone tissue engineering in a rotating bioreactor using a microcarrier matrix system. J Biomed Mater Res 2001, 55: 242–253.
17 Saini S and Wick TM. Concentric cylinder bioreactor for production of tissue engineered cartilage: effect of seeding density and hydrodynamic loading on construct development. Biotechnol Prog 2003, 19: 510–521.
18 Grayson WL, Marolt D, Bhumiratana S, Fröhlich M, Guo XE and Vunjak-Novakovic G. Optimizing the medium perfusion rate in bone tissue engineering bioreactors. Biotechnol Bioeng 2011, 108: 1159–1170.
19 Goldstein AS, Juarez TM, Helmke CD, Gustin MC and Mikos AG. Effect of convection on osteoblastic cell growth and function in biodegradable polymer foam scaffolds. Biomaterials 2001, 22: 1279–1288.
20 Beck GR, Zerler B and Moran E. Phosphate is a specific signal for induction of osteopontin gene expression. Proc Natl Acad Sci USA 2000, 97: 8352.
21 Mahalingam CD, Datta T, Patil RV, Kreider J, Bonfil RD, Kirkwood KL and Goldstein SA, *et al*. Mitogen-activated protein kinase phosphatase 1 regulates bone mass, osteoblast gene expression, and responsiveness to parathyroid hormone. J Endocrinol 2011, 211: 145–156.
22 Schofer MD, Veltum A, Theisen C, Chen F, Agarwal S, Fuchs-Winkelmann S and Paletta JR. Functionalisation of PLLA nanofiber scaffolds using a possible cooperative effect between collagen type I and BMP-2: impact on growth and osteogenic differentiation of human mesenchymal stem cells. J Mater Sci Mater Med 2011, 22: 1753–1762.
23 Stangenberg L, Schaefer DJ, Buettner O, Ohnolz J, Möbest D, Horch RE and Stark GB, *et al*. Differentiation of osteoblasts in three-dimensional culture in processed cancellous bone matrix: quantitative analysis of gene expression based on real-time reverse transcription-polymerase chain reaction. Tissue Eng 2005, 11: 855–864.
24 Lagari VS and Levis S. Phytoestrogens and bone health. Curr Opin Endocrinol Diabetes Obes 2010, 17: 546–553.
25 Somjen D, Kohen F, Lieberherr M, Gayer B, Schejter E, Katzburg S and Limor R. Membranal effects of phytoestrogens and carboxy derivatives of phytoestrogens on human vascular and bone cells: new insights based on studies with carboxy-biochanin A. J Steroid Biochem Mol Biol 2005, 93: 293–303.
26 Knight DC and Eden JA. A review of the clinical effects of phytoestrogens. Obstet Gynecol 1996, 87: 897–904.
27 Boyce BF and Xing L. Functions of RANKL/RANK/OPG in bone modeling and remodeling. Arch Biochem Biophys 2008, 473: 139–146.
28 Sanchez C, Gabay O, Salvat C, Henrotin YE and Berenbaum F. Mechanical loading highly increases IL-6 production and decreases OPG expression by osteoblasts. Osteoarthritis Cartilage 2009, 17: 473–481.
29 Kreja L, Liedert A, Hasni S, Claes L and Ignatius A. Mechanical regulation of osteoclastic genes in human osteoblasts. Biochem Biophys Res Commun 2008, 368: 582–587.
30 Chi Hyun K, Lidan Y and Clare E. Oscillatory fluid flow-induced shear stress decreases osteoclastogenesis. Bone 2006, 39: 1043–1047.
31 Schindler M, Nur-E-Kamal A, Ahmed I, Kamal J, Liu HY, Amor N and Ponery AS, *et al*. Living in three dimensions. Cell Biochem Biophys 2006, 45: 215–227.
32 Liu L, Zhang XZ and Deng GR. Advances in research of cell models for osteoporosis drug screening. Chin J Pharm 2011, 46: 406–409.